Emergent Materials
https://doi.org/10.1007/s42247-024-00907-7

ORIGINAL ARTICLE

Light-responsive liposome as a smart vehicle for the delivery of anticancer herbal medicine to skin

Atefeh Zarepour[1,2] · Zeynep Ülker[3,4] · Arezoo Khosravi[5] · Abdurrahman Coskun[6] · Yavuz Nuri Ertas[7,8] · Mehmet Yildiz[3] · Ali Zarrabi[2,9]

Received: 23 July 2024 / Accepted: 8 October 2024

Abstract

Sunlight is composed of various wavelengths, including visible light, ultraviolet (UV) rays, and infrared radiation that serves as a double-edged sword for humans via providing the energy for sustaining life on Earth and also acting as a source of hazardous UV radiation. The skin, as the largest protective part of the body, is exposed to sunlight daily, making it critical to protect this organ from its harmful effects. Accordingly, this research aims to fabricate a new type of light-responsive liposome to deliver herbal medicine as protective compounds with antioxidant and anticancer properties. The light-responsive part of this liposome has the capability of cleavage after exposure to UV-A light (the main UV-parts of sunlight) and improves drug release pattern. In detail, a light-responsive compound was fabricated at first and then was used along with phospholipids and curcumin (a type of herbal drug)-loaded cyclodextrin for the fabrication of liposomes using the thin-film hydration method. The physicochemical analysis confirmed the fabrication of spherical liposomes approximately 145 nm in size, which released around 62% of the therapeutic cargo over 120 h when exposed to UV irradiation. Besides, it showed anticancer ability (against melanoma cancer cells) while having a protecting effect for the normal cell line. Therefore, it could be a candidate for further application in skin-protecting products like wound healing compounds or anticancer usage.

Keywords Smart drug delivery · Liposome · Antioxidant · Herbal medicine · Anticancer

✉ Yavuz Nuri Ertas
yavuzertas@erciyes.edu.tr

✉ Mehmet Yildiz
mehmet.yildiz@sabanciuniv.edu

✉ Ali Zarrabi
ali.zarrabi@istinye.edu.tr

Atefeh Zarepour
atefeh.zarepour@gmail.com

Zeynep Ülker
zeynep.1.ulker@kcl.ac.uk

Arezoo Khosravi
arezoo.khosravi@okan.edu.tr

Abdurrahman Coskun
abdurrahman.coskun@acibadem.edu.tr

[1] Department of Research Analytics, Saveetha Institute of Medical and Technical Sciences, Saveetha Dental College and Hospitals, Saveetha University, Chennai 600 077, India

[2] Department of Biomedical Engineering, Faculty of Engineering and Natural Sciences, Istinye University, 34396 Istanbul, Turkey

[3] Faculty of Engineering and Natural Sciences, Sabanci University, 34956 Istanbul, Turkey

[4] Faculty of Life Sciences & Medicine, King's College London, SE1 8WA London, England, UK

[5] Department of Genetics and Bioengineering, Faculty of Engineering and Natural Sciences, Istanbul Okan University, 34959 Istanbul, Turkey

[6] Department of Medical Biochemistry, School of Medicine, Acibadem Mehmet Ali Aydinlar University, 34752 Ataşehir, Istanbul, Turkey

[7] Department of Biomedical Engineering, Erciyes University, 38039 Kayseri, Turkey

[8] Department of Technical Sciences, Western Caspian University, AZ1001 Baku, Azerbaijan

[9] Graduate School of Biotechnology and Bioengineering, Yuan Ze University, Taoyuan 320315, Taiwan

Published online: 21 November 2024

1 Introduction

Skin is the largest organ of the body, acting as the first defense line against external harmful factors such as pathogens, UV radiation, and environmental pollutants. Besides, it contributes to the regulation of body temperature, synthesis of vitamin D, and sensation. Skin health is closely associated with psychological well-being, impacting self-esteem and quality of life [1–3]. The aging of this organ results from intrinsic and extrinsic factors that could affect its functions. One of the main reasons for skin aging is oxidative stress resulting from the production of reactive oxygen species (ROS) inside cells due to various factors such as exposure to UV radiation, pollution, smoking, and metabolic processes within the body [4]. One of the most important natural sources of UV radiation is sunlight that is exposed to our body's skin each day. Melanoma, a relatively rare and aggressive form of skin cancer, accounts for only 1% of total reported cases but presents a notably higher fatality rate. It is revealed in the literature that exposure to UV radiation (both A and B types) from the sun could not only produce ROS but also improve the probable occurrence of melanoma skin cancer via inducing DNA mutation. Delayed diagnosis results in its metastasis to other body regions and can culminate in a distressing outcome [5, 6]. This makes it important to find and introduce new methods for overcoming these side effects of sunlight.

Herbal medicine is one class of therapeutic compounds that could be used for different purposes, from antibacterial and anti-inflammatory to anticancer activity. Indeed, herbal medicine is the oldest therapeutic method used by humans for at least 5000 years.Moreover, the presence of various compounds in herbal medicine enables it to exhibit multi-therapeutic effects simultaneously, with fewer side effects than other active therapeutic methods. In the case of skin and wounds, the application of herbal medicine gained significant attention these days due to their natural origin [7, 8].

Curcumin is a type of flavoring agent derived from the rhizomes of *Curcuma longa* that is used in several studies as a common type of herbal medicine. It is accepted by the US Food and Drug Administration (FDA) as a safe material and shows several interesting features, including anti-microbial, antioxidant, anti-diabetic, anti-inflammatory, anti-proliferative, anti-cancer, and wound healing capabilities [9–11]. It could do its different roles via activating or suppressing different intracellular pathways and compounds; for instance, it could induce antioxidant activity via downregulating the expression levels of inflammatory factors like nuclear factor kappa-light-chain-enhancer of activated B cells (NF-κB), tumor necrosis factor (TNF α), and interleukins. In the case of wound healing, curcumin could suppress inflammation conditions, exhibit antibacterial activity, and accelerate healing process via inducing proliferation of fibroblast cells, neoangiogenesis, and upregulating collagen deposition [12, 13]. However, its low water solubility reduces its widespread application and makes it important to use a nanocarrier to mask this compound and deliver it to its targeted site.

Since their discovery in the 1960s [14], liposomes have been extensively studied as cell membrane models due to their similarity to the lipid bilayer of cells. These spherical nanostructures comprise various phospholipids and cholesterol, strategically organized to possess a hydrophilic core and a hydrophobic bilayer (attributed to the presence of cholesterol and phospholipid tails) [15, 16]. Due to their interesting properties such as biocompatibility, ease of synthesis, biodegradability, non-immunogenicity, bioavailability, and modifiability, liposomes have been widely used as drug delivery vehicles. Notably, their structural characteristics make them well-suited for encapsulating both hydrophobic and hydrophilic therapeutic compounds. Consequently, this encapsulation enhances drug bioavailability, shields compounds from degradation, augments stability, and through targeted delivery, elevates therapeutic efficacy while mitigating side effects on other tissues [17–20].

Light-responsive liposomes, a subclass of smart liposomal nanocarriers, show promising results in revolutionizing targeted drug delivery. Engineering the structure of these liposomes allows them to respond to external light stimuli, offering precise spatiotemporal control over drug release. Indeed, utilizing light-sensitive components (such as photoactive molecules or light-triggered mechanisms) in the structure of these compounds enables the on-demand release of encapsulated therapeutic agents. This capability facilitates fine-tuning of drug administration, minimizing systemic side effects and enhancing therapeutic efficacy [21].

The photoresponsive process used by the materials is divided into four main mechanisms: photoisomerization, photocleavage, photocrosslinking, and photoinduced rearrangement. According to these mechanisms, different materials have been introduced; among them is the family of nitrobenzyl alcohol, which uses photo-cleavage mechanisms after being exposed to UV radiation in the range of 320–400 nm (ultraviolet A (UV-A)) [22]. Most of the UV sunlight that arrives on the earth is in the range of UV-A (95%), which could penetrate the dermis part of the skin [23], so it could be a natural source for the degradation of light-responsive compounds containing nitrobenzyl alcohol in their structure.

According to the above-mentioned features, this research aims to fabricate a new type of light-responsive liposome with the ability to load curcumin and release it in response to UV-A light. Therefore, at first, we fabricated a new type of light-responsive compound. Curcumin molecules were

then loaded inside the cavity of the cyclodextrin compound to improve its bioavailability and sustained release pattern. Then, these compounds along with phospholipids were applied to produce liposomes via the thin-film hydration method. In order to synthesize liposome nanoparticles, we used soy-lecithin phospholipid as the main compound, which is a natural compound derived from a renewable source through a more ecologically friendly process and has less toxicity effects [24]. After the production of liposomes, different types of physicochemical and biological tests were applied to evaluate the characteristic features of fabricated liposomes, confirm their light-responsive ability, and check their application for anticancer purposes.

2 Materials and methods

2.1 Materials

L-α-Phosphatidylcholine (PC), cholesterol, succinic anhydride, penicillin-streptomycin, phosphate-buffered saline (PBS), 4-dimethylaminopyridine (DMAP), HCl, chloroform, dimethyl sulfoxide (DMSO), methanol, β-cyclodextrin, acetone, 3-(4,5-dimethylthiazol-2-yl)-2,5-diphenyl tetrazolium bromide (MTT), and curcumin were purchased from Sigma. 2-Nitrobenzyl alcohol (NBA) was purchased from Alfa Aesar. 1,2-Distearoyl-sn-glycero-3-phosphorylethanolamine (DSPE) and 2′,7′-Dichlorofluorescein diacetate were bought from Cayman. Dulbecco's Modified Eagle Medium (DMEM), fetal bovine serum (FBS), and trypsin-EDTA were purchased from Biowest. NIH/3T3 and B16F10 cell lines were received from ATCC.

2.2 Method

2.2.1 Fabrication of light-responsive compound (2-nitrobenzyl succinate@cholesterol (NBS@Chol))

A two-step reaction was employed to prepare NBS@cholesterol. Initially, a mixture of 500 mg of succinic anhydride (SA) and 383 mg of 2-nitrobenzyl alcohol (NBA) was dissolved in 20 ml of chloroform. Subsequently, 153 mg of 4-dimethylaminopyridine (DMAP) was added to the solution, and the resulting mixture was refluxed at 60 °C under a nitrogen (N_2) atmosphere for 24 h. The solvent was then removed using a rotary evaporator. The obtained precipitate underwent washing three times with 10% hydrochloric acid (HCl) and extraction with saturated sodium bicarbonate ($NaHCO_3$). Diethyl ether was introduced into the basic solution, followed by adjusting the pH to approximately 5 using 10% HCl. The sample was refrigerated overnight at 4 °C to facilitate the collection of the resulting white precipitate. Subsequently, the product (NBS) was dried overnight at 40 °C. Notably, the entire process was conducted under dark conditions [25, 26].

In the second step, cholesterol was introduced into a 15 ml solution of anhydrous dichloromethane (DCM), followed by the addition of 417 µl of triethylamine. The resulting solution was stirred for a few minutes under a nitrogen (N_2) atmosphere. Subsequently, the reaction temperature was reduced to 0 °C, and NBS (dissolved in DCM) was added dropwise to the solution while stirring at 0 °C for 1 h. Stirring continued for an additional 24 h at room temperature. The solvent was then removed using a rotary evaporator, and the residue was washed with cold ethanol before undergoing recrystallization, resulting in the formation of a yellow pellet [27].

2.2.2 Fabrication of curcumin-loaded cyclodextrin (Cur@Cyclo)

74 mg of curcumin was dissolved in 5 mL of acetone and added dropwise to an aqueous solution containing 230 mg of β-cyclodextrin in 20 mL. The resulting solution was stirred at room temperature for 24 h, followed by centrifugation. The supernatant was collected and subsequently dried using a freeze-dryer for 48 h.

2.2.3 Fabrication of light-responsive liposome

A combination of PC, DSPE, and NBS@Chol, with approximate weights of 4 mg, 0.6 mg, and 1.3 mg, respectively, was employed to fabricate light-responsive liposomes utilizing the thin-film hydration method. Initially, these components were accurately weighed and dissolved in a 3 mL mixed solution of methanol and chloroform at a 1:1 ratio. The solvent was subsequently evaporated using a rotary evaporator at 40 °C for 1 h. Hydration of the thin film was achieved by adding 4.5 mL of phosphate-buffered saline (PBS) to the formed thin film, followed by sonication for 1 h at 40 °C. The resultant liposomes were then stored at 4 °C for subsequent analysis. The same methodology was applied for the production of drug-loaded liposomes by dissolving 3 mg of Cur@Cyclo in PBS and introducing this solution to the thin-film layer during fabrication.

2.2.4 Characteristic analysis

The size and surface charge of the nanoparticles were determined using a Zeta Analyzer (Malvern Panalytical, Zetasizer Nano ZS). Liposomes were dissolved in 3 mL of water and sonicated for 30 min. Subsequently, the hydrodynamic size of the particles and their surface charge were measured using dynamic light scattering (DLS) and zeta

potential, respectively. DLS was also employed to confirm the light-responsiveness of the nanoparticles by measuring their size before and after 30 min irradiation with 365 nm UVlight. Surface functional groups of the fabricated compounds were characterized using Fourier transform infrared spectroscopy (FTIR, Jasco, FT/IR 4600). Small amounts of each material were used for the measurements conducted between the wavenumbers of 500–4000 cm^{-1}. Particle size was further assessed using scanning transmission electron microscopy (STEM, Thermoscientific, Quattro S) and field emission scanning electron microscopy (FE-SEM, GeminiSEM 500, ZIESS, Germany). The crystal structure of the compounds was determined using X-ray Diffraction (XRD, Malvern Panalytical Empyrean, UK) spectroscopy within the range of $2\theta = 5–55°$. Additionally, the drug loading amount and release pattern were evaluated using UV-Visible spectroscopy (Jasco, V-730 BIO) at 430 nm. To this end, drug-loaded liposomes were centrifuged at 9000 RPM for 20 min to precipitate liposomes. The supernatant was separated, and 1 ml of PBS was added to the precipitate, and the suspension was centrifuged again. The absorbance of total supernatant was measured by UV-Visible as the non-loaded drug, and then the percentage of entrapment efficiency was calculated via comparing the amounts of loaded drug with total used amounts.

For the drug release test, two samples with identical concentrations were prepared; one of them was exposed to UV radiation (365 nm) for 10 min, while the other one was kept in the dark. Both samples were incubated at 37 °C for 120 h. At specific intervals, 100 µL of each sample was collected, mixed with 900 µL of acetone, and their absorbance was measured using UV-Visible spectroscopy. Then, the drug release kinetics were checked, and release models were determined.

2.2.5 Cell viability and anticancer assessment

The 3-(4,5-dimethylthiazol-2-yl)-2,5-diphenyl tetrazolium bromide (MTT) assay was employed to assess the cytocompatibility and anticancer effects of drug-loaded liposomes in both presence and absence of light. NIH/3T3 fibroblast cells were utilized to evaluate sample cytocompatibility, while the anticancer efficacy was evaluated against B16F10 melanoma cancer cells. Initially, 10^4 cells were seeded into each well of a 96-well plate and incubated at 37 °C for 24 h. Subsequently, two sets of liposomal nanoparticle solutions with different concentrations (100, 50, 25, 12.5, and 6.25 µg/mL) in media were prepared. One set was exposed to UV radiation for 10 min, while the other was shielded from light exposure and added to the cells. After 48 h, the culture medium was removed, cells were washed with PBS, and a fresh medium containing MTT solution (5 mg/mL in PBS) was added to each well, followed by incubation at 37 °C for 4 h. Thereafter, the medium was replaced with 100 µL of dimethyl sulfoxide (DMSO), and after 1 h of incubation at 37 °C in a dark environment, the absorbance of each well was measured using a microplate reader (SPECTROstar, Nano) at 570 nm. Each sample was tested in triplicate, and cells combined with media served as the control.

2.3 Statistical analysis

Results of MTT assay were statistically assessed using SPSS software (version 27, parametric analysis of variance [ANOVA (Tukey)]) by considering $P_{value} \leq 0.05$ as significancy.

3 Results and discussion

3.1 Fabrication of curcumin-loaded cyclodextrin

Different physicochemical tests were used to confirm the fabrication of the curcumin-β-cyclodextrin inclusion complex, which are described in the following. First of all, we employed FTIR analysis to assess the formation of the inclusion complex (Fig. 1a). According to the results of this test, the broad band between 3000 and 3500 cm^{-1} and bands between 2850 and 3000 cm^{-1} in the spectrum of β-cyclodextrin were attributed to the vibration of OH and CH groups, respectively. Besides, bands at 845, 1016, and 1628 cm^{-1} were related to the C-O-C of cyclodextrin rings, stretching of glucose units, and H-OH groups, respectively [28]. In the spectrum of curcumin, bands at around 3500, 1624, 1507, 1425, 1270, and 1016 cm^{-1} were attributed to the stretching vibration of OH, benzene ring, C=O (and C=C), C-H, C-O, and C-O-C groups of this compound [29]. The spectrum of curcumin-loaded cyclodextrin showed most of the peaks related to the cyclodextrin, while some of the main peaks of curcumin (two weak peaks at around 1624 and 1507 cm^{-1} that were related to the benzene ring and carbonyl groups, respectively, peaks between 2800 and 2900 cm^{-1} that were attributed to the alkyl groups, and a peak at 1425 cm^{-1} related to the ether group) could be observed as well. Therefore, it could be concluded that curcumin compounds were encapsulated inside the cyclodextrin cavity.

Results of XRD analysis (Fig. 1b) showed some differences between the spectrum of inclusion complex and that of cyclodextrin and curcumin alone, such as the appearance of a new peak at around $2\theta = 6.63^{\circ}$ along with the changes in the intensity of other peaks, all of which could confirm the formation of inclusion complex [30, 31].

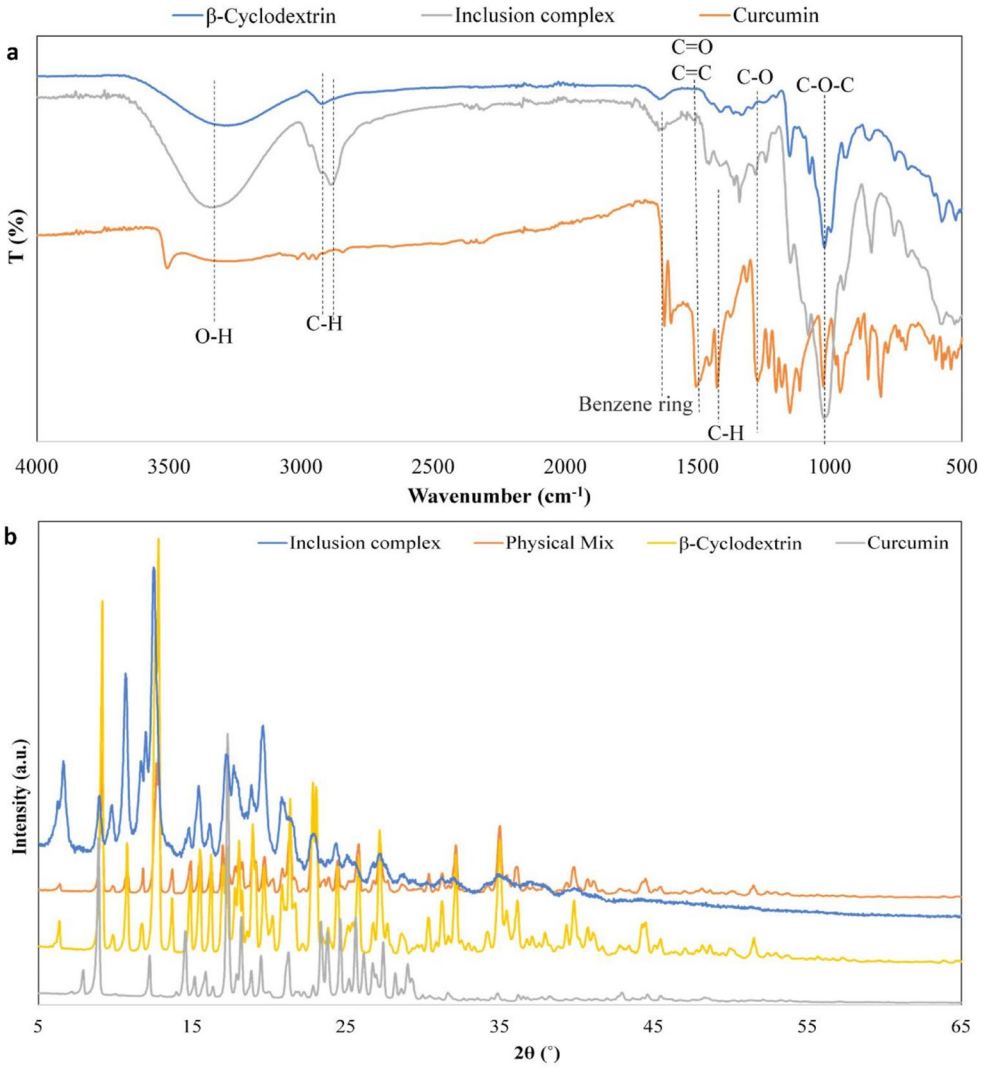

Fig. 1 (**a**) FTIR results of curcumin, inclusion complex, and β-cyclodextrin (**b**) XRD results of curcumin, β-cyclodextrin, physical mixture, and inclusion complex

Results of FESEM analysis also confirmed the fabrication of inclusion complexes due to the clear differences between their electron microscopy analysis (Fig. 2a). Besides they fabricated aggregate structures with a size near 20 nm (Fig. 2b).

3.2 Liposome preparation

3.2.1 Fabrication of light-responsive compounds

For the preparation of the light-responsive component, a two-step reaction is realized during which carboxylate NBA (NBS) is fabricated at first and then this compound is attached to cholesterol (Scheme 1).

To confirm the occurrences of this process, FTIR analysis was performed after each step, with their respective results depicted in Fig. 3. In the spectrum of NBS, peaks observed at approximately 1730 cm^{-1}, 1160 cm^{-1}, and 1700 cm^{-1} were attributed to the C = O and C-O of ester and C = O of carboxylic acid groups, respectively, thereby confirming the successful conjugation of NBA and succinic anhydride. Additionally, the presence of an OH peak of NBS around 3052 cm^{-1} (similar to succinic anhydride) and distinct peaks at approximately 1333 cm^{-1} and 1512 cm^{-1}, corresponding to the nitrobenzyl compound, substantiated the presence of both components in the structure of the final product. The absence of a peak related to the OH group of primary alcohol (typically located around 1033 cm^{-1}), coupled with the presence of peaks associated with the NO group in the structure of NBS, confirmed the conjugation of succinic anhydride to the NBA through interaction between the alcohol and acid groups of these components (Fig. 3a).

In the next step, conjugation between cholesterol and NBS was checked via FTIR (Fig. 3b). The occurrence of conjugation was confirmed by the disappearance of peak related to the carboxylic acid group (compared to the NBS and physical mixture) and the creation of peaks related to the cholesterol (OH vibration between 3200 and 3500 cm^{-1},

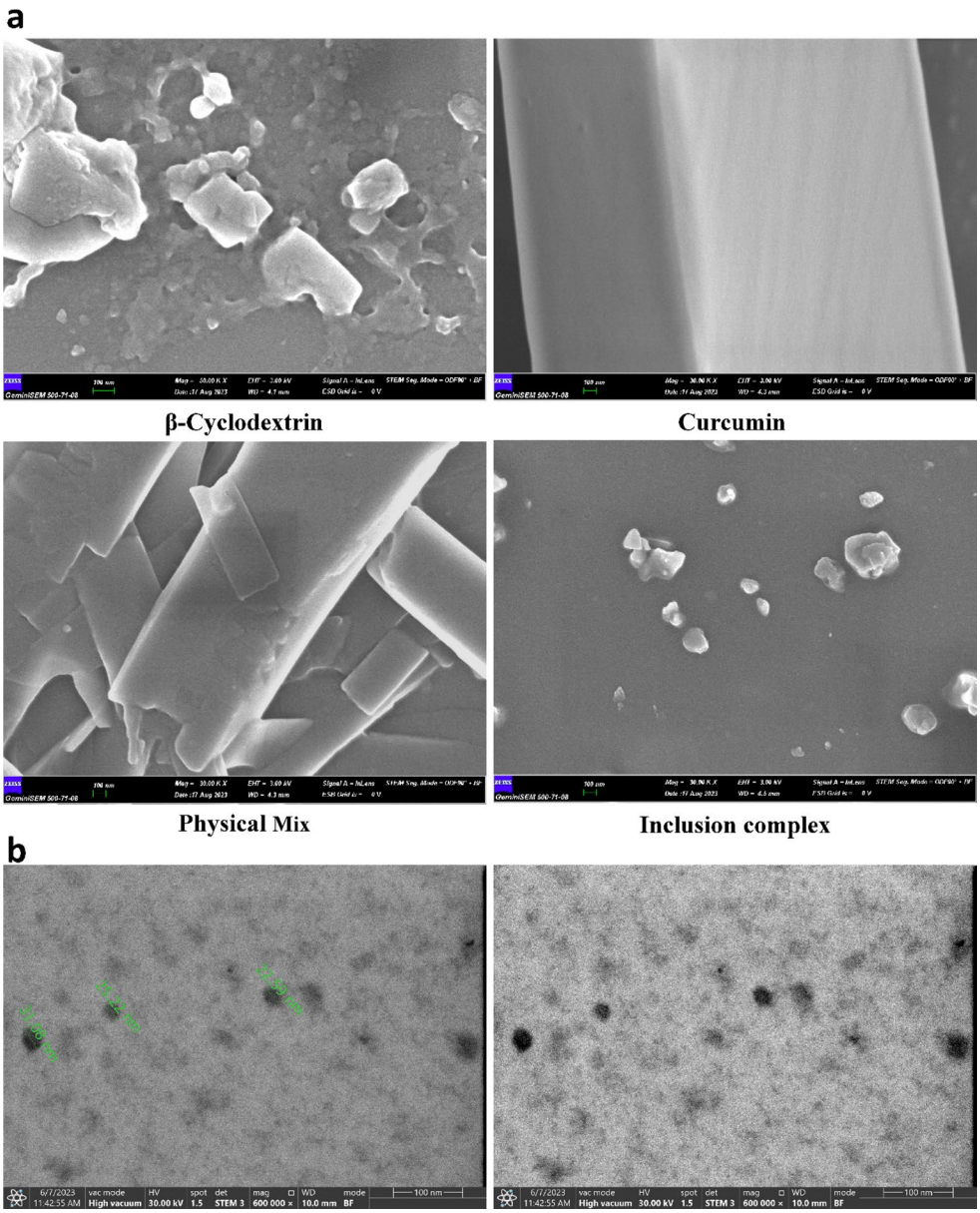

Fig. 2 (**a**) FESEM image of β-cyclodextrin, curcumin, their physical mixture, and their inclusion complex (**b**) STEM image of inclusion complex (Scale bar = 100 nm)

CH between 2800 and 2950, 1478 and 1363 cm^{-1}, and CO stretching vibrations at around 1035 cm^{-1}) [32] in the spectrum of conjugated structure.

3.2.2 Synthesis of drug-loaded smart liposome

FTIR In the next step, this compound along with phospholipids and drug-loaded cyclodextrin was used for the fabrication of liposomes. FTIR results of liposome (with/without curcumin@cyclodextrin) showed characteristic peaks at around 3400, 2800–2900, 1740, and 1057 cm^{-1}, which are related to the stretching vibration of OH, CH, C=O, C-O (or C-C) of cholesterol and lecithin, as the main components of liposome (Fig. 4) [33, 34]. By comparing the spectrum of drug-loaded liposomes with the spectrum of bare liposomes and also curcumin-loaded cyclodextrin, we could confirm the presence of cyclodextrin inside the liposomes, since some of the characteristic peaks related to this material (between 900 and 1200 cm^{-1}) are evident in the spectrum of drug-loaded liposomes as well. Moreover, given the differences in the spectra of liposomes containing cyclodextrin and free cyclodextrin, we could infer that these particles are encapsulated within the core of the liposomes rather than being present on the surface.

DLS and Zeta potential The size and Zeta potential of the fabricated liposomes with/without therapeutic compound were measured to determine their hydrodynamic size and surface charge. Table 1 shows the results of DLS and zeta analysis of the liposomes with/without therapeutic

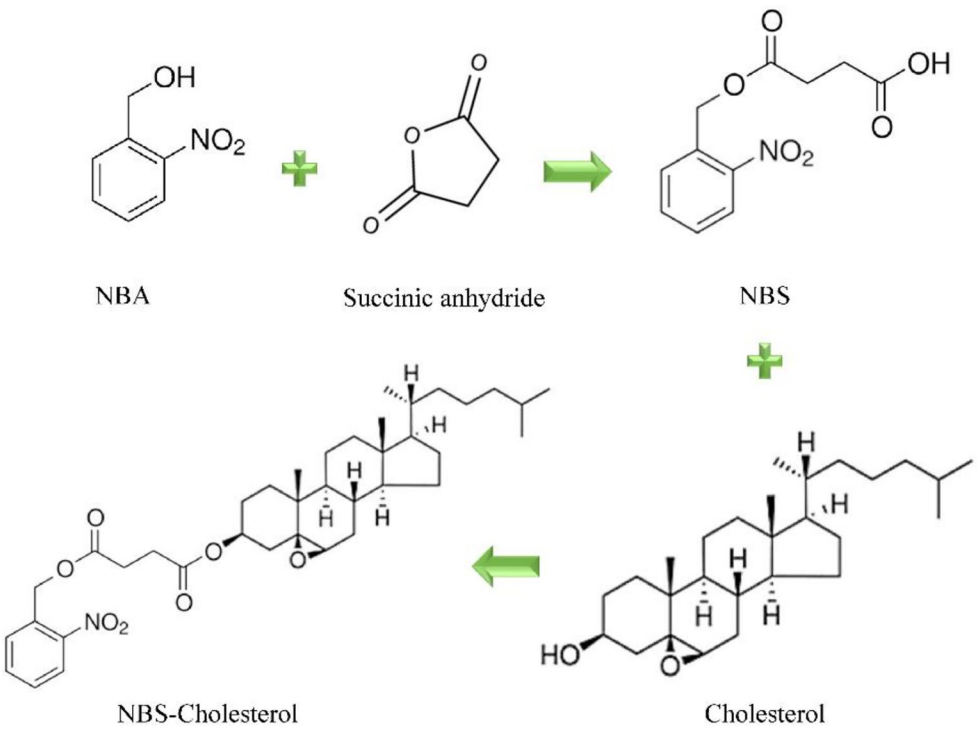

Scheme 1 Chemical process related to the fabrication of light-responsive compound (NBS-Cholesterol)

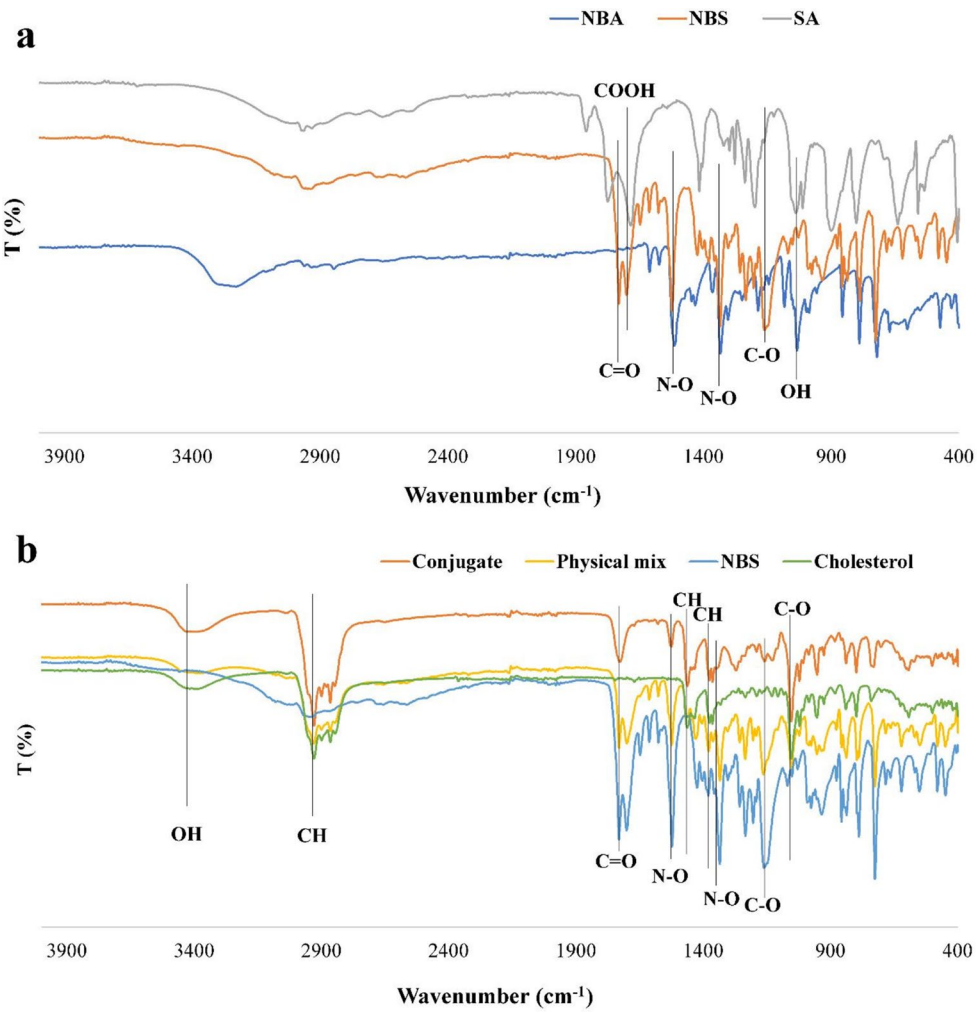

Fig. 3 FTIR results related to the fabrication of (**a**) NBS, and (**b**) light-responsive cholesterol

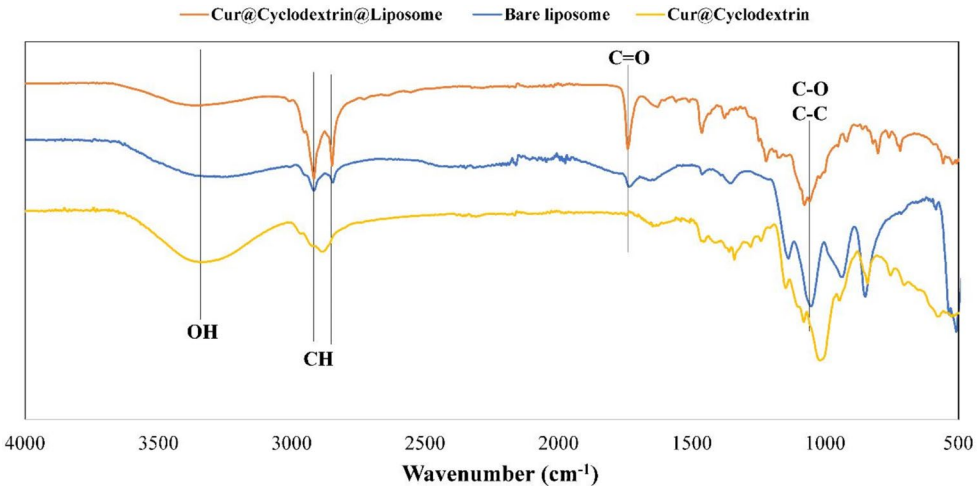

Fig. 4 FTIR spectrum of liposomes with/ without curcumin-loaded cyclodextrin compound

Table 1 Results of DLS and Zeta analysis of bare liposome, liposome-loaded drug, and liposome-loaded drug exposed with UV-light for 30 min

Sample	DLS (nm)	Zeta potential (mV)	PDI	Encapsulation efficiency (%)
Bare liposome	145.66 ± 15	-35	0.282 ± 0.022	-
Drug-loaded liposome	135.5 ± 20	-36	0.185 ± 0.015	84
Drug-loaded liposome treated with UV radiation	169.2± 17.51	-38.63	0.297	-

compounds. According to the results of these tests, bare liposomes had a slightly larger size than the drug-loaded ones. Besides, drug-loaded samples showed better PDI in comparison to the bare liposome, indicating that drug-loaded samples had more monodispersed particles, which may be due to the presence of therapeutic compounds. The same results were seen in some of the other research [35, 36]. In the case of surface charge, both samples showed the same high negative surface charge that could lead to their stability. The negative charge observed may be attributed to the presence of cholesterol in the liposome structure, causing a reorientation of phospholipids wherein their negative charges are directed towards the outer part. Besides, the main compound of these liposomes is lecithin, which has a negatively charged phosphocholine group [37, 38].

Additionally, we employed DLS and Zeta analysis to assess the light responsiveness of the fabricated liposomes. We initially measured the size and charge of the liposomes and subsequently exposed them to UV radiation (365 nm) for 30 min before re-evaluating their size and charge. Interestingly, the nanoparticles exhibited an increase in both size and PDI after UV irradiation. Additionally, a new peak emerged in the sample spectrum, confirming the light-responsive nature of the fabricated liposomes. Furthermore, the particle charge decreased after irradiation, potentially indicating the formation of carboxylic acid groups due to the degradation of the connection between NBA and cholesterol.

STEM The morphology and size of the drug-loaded nanoliposomes were determined through STEM analysis (Fig. 5). As per the STEM results, the size of nanoparticles was about 145 ± 10 nm, which is nearly similar to the size measured by the DLS. Furthermore, the STEM analysis allowed us to observe the width of both the core (appearing dark, possibly due to the presence of curcumin and its fluorescence effect) and the shell of the nanoparticles. This observation further confirmed the encapsulation of curcumin-loaded cyclodextrin within the core of the liposome, corroborating the findings obtained earlier through FTIR analysis.

3.2.3 Drug loading and release

The fabricated liposomes exhibited an entrapment efficiency of approximately 84%, as detailed in Table 1. Figure 6 shows the drug release pattern of light-responsive liposomes. For this experiment, the fabricated liposomes were divided into two groups: one exposed to UV radiation for 10 min, and the other covered with aluminum foil to mitigate light exposure. Both samples were then maintained at 37 °C for 120 h, with drug release measurements taken at specific time intervals. According to the results of drug release, both samples showed a three-step drug release pattern. This pattern included an initial rapid release (within the first 24 h), followed by a gradual release (between days 1 and 3), and a subsequent rapid release. As could be seen

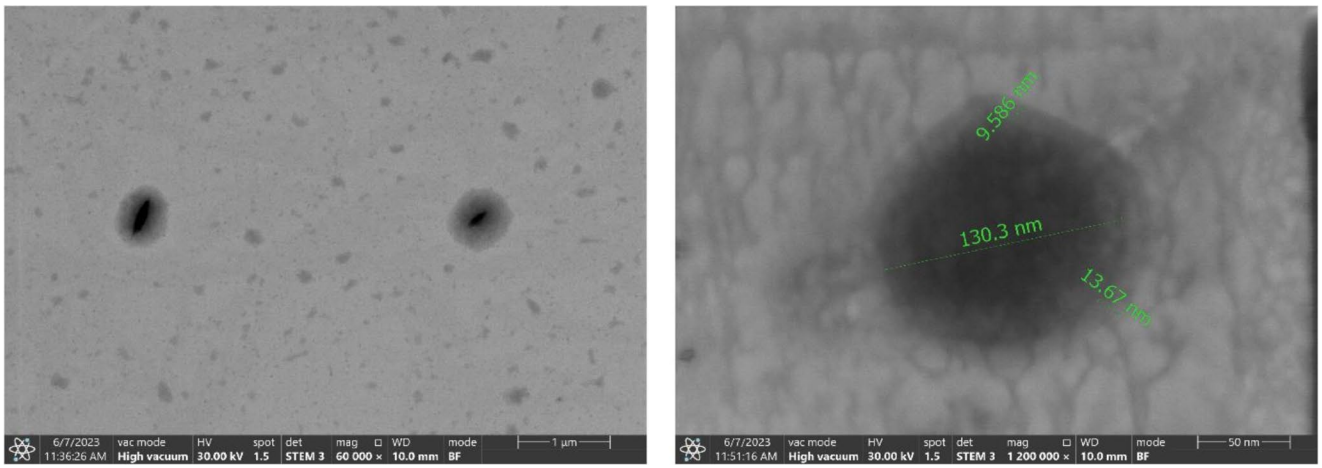

Fig. 5 STEM image of drug-loaded nanoliposomes

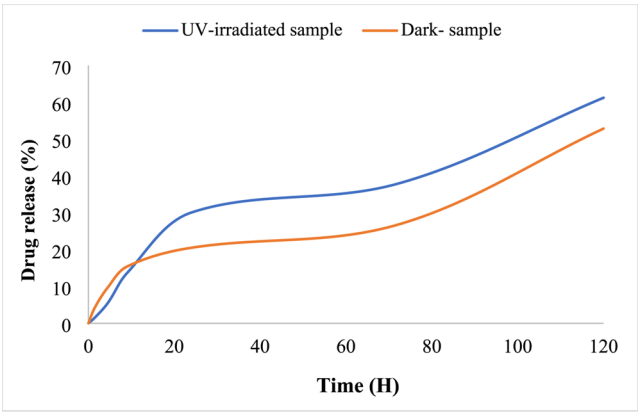

Fig. 6 Drug release pattern of light-responsive liposome in dark and after exposure to UV-light

Table 2 Different kinetic models used for drug released in different conditions

Models/Samples	R^2 value	
	UV irradiated sample	Dark sample
Zero order	0.9188	0.9182
First order	0.1700	0.1460
Hickson-Crowel	0.6363	0.5627
Higuchi	-0.6169	-0.6430

in the figure, throughout all three steps, the UV-irradiated sample exhibited higher levels of drug release, thereby confirming the effectiveness of using the light-responsive compound. We hypothesize that in the second step, drug-loaded cyclodextrin is released from liposomes, followed by the release of curcumin from cyclodextrin in the third step, leading to another rapid release phase. Consequently, the incorporation of cyclodextrin in the liposome structure provides control over drug release. Moreover, the simultaneous use of these two types of drug delivery vehicles combines their beneficial effects [39]. In comparison to other types of lipid-based delivery systems like solid lipid nanoparticles (SLN), this formulation showed a more controllable release profile so that it could release about 60% of its therapeutic cargo within 120 h, while in SLN produced by Rapalli et al., 100% of the drug was released within 48 h, which is very fast [40].

Four different models were used to evaluate the kinetics of releasing process, including zero order, first order, Higuchi, and Hixson-Crowell models (Table 2). According to the results of the kinetic study, both samples showed zero order model (with a higher R^2 value). This model offers a solution to the challenges associated with rapid release by providing a consistent drug release rate. This approach helps sustain the drug levels within the therapeutic range for a longer duration, potentially minimizing side effects, decreasing the need for frequent dosing, and enhancing patient adherence to treatment [41].

3.2.4 Cell viability assessment

MTT assay was used to determine the effect of drug-loaded light-responsive liposomes on normal and melanoma cancer cells and to confirm its cytocompatibility and anticancer effect. Figure 7 shows the results of the MTT test on 3T3 fibroblast and B16F10 cancer cells. According to the results of this test, the fabricated liposomes demonstrated excellent cytocompatibility, showing no toxicity and even enhancing the viability of normal cells in some cases. This is consistent with other studies that reported similar cytocompatibility profiles for liposomal formulations, underscoring their potential for safe clinical applications. On the other hand, they showed more than 30% toxicity effects against melanoma cancer cells, even in low concentrations (12.5 µg/mL). Moreover, exposure to UV radiation slightly increased the toxicity effects of the liposomes, potentially due to enhanced drug release triggered by UV irradiation. This observation suggests that UV activation can be fine-tuned to

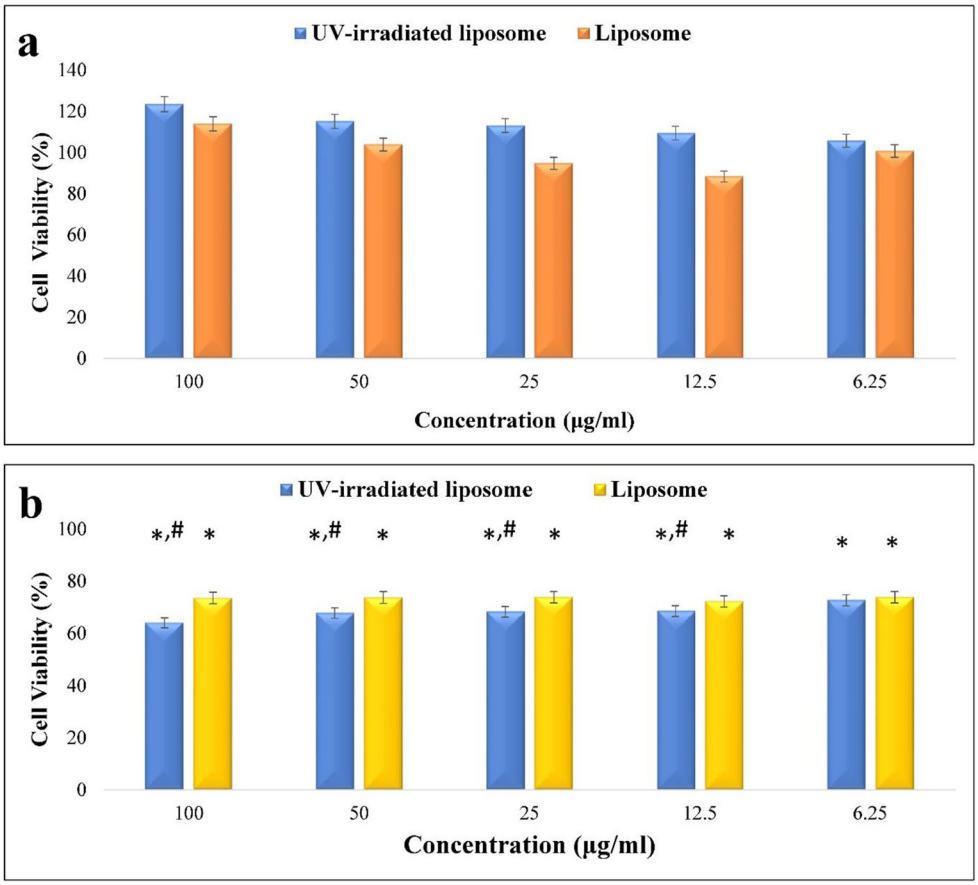

Fig. 7 Results of MTT assay against (**a**) 3T3 fibroblast cells, and (**b**) B16F10 Melanoma cancer cells (* and # are related to the $P_{value} \leq 0.05$ for samples compared with control and non-irradiated samples, respectively)

optimize therapeutic outcomes, although further studies are needed to fully understand the underlying mechanisms and potential side effects. These findings confirm the anticancer capabilities of the fabricated liposomes, positioning them as a potential delivery vehicle for skin cancer treatment.

There are different studies in which different types of liposomes were fabricated and loaded with curcumin (and other therapeutic compounds) and were used for cancer treatment [42–46]. In this context, different strategies were used to enhance the therapeutic performance of these therapeutic formulations. For instance, glycyrrhetinic acid-modified curcumin-loaded cationic liposome (GAMCLCL) was introduced by Chang et al. that exhibited better anticancer activity in comparison with free curcumin [47]. In another study, liposomes functionalized with galactose-morpholine were fabricated that had the capability of targeting the hepatoma cells (because of galactose) and lysosome (because of morpholine). This formulation showed near 61% drug release within 24 h, which was faster than this work and could reveal a more controllable release profile of this work. Besides, the targeted liposome did not show significant toxicity effect on HepG2 cells, while it could reduce the size of tumor tissue in an in vivo test [48]. While in this work, we could see a significant cytotoxicity effect on cancer cells and no toxicity result on normal cell line.

Folic acid-targeted liposome was used in another study that showed about 80% entrapment efficiency with a size of about 138 nm (nearly the same as this work) and controllable release of drug (about 50%) within 72 h. It also showed more than 80% toxicity effect against cancer cells after 48 h of incubation at 50 µM of curcumin [43]. A smart pH-responsive liposome was fabricated in another study and used for the treatment of breast cancer. Compared to the normal liposome, the smart type liposome showed more controllable drug release pattern within 120 h, better stability during 3 months, and more cytotoxicity effect [49]. It is evident that modifying the structure of liposomes is an ideal method to enhance their therapeutic performance. In this research, we introduced a novel form of light-responsive liposome loaded with curcumin to be applied as a protective compound against the hazardous effects of UV radiation. Despite the good results that were achieved during this research, more and more research (in vitro and in vivo) should be done on it to find out all of its properties and improve its therapeutic performance.

4 Conclusion

In this study, we developed a new type of smart light-responsive liposomal nanoparticles capable of being activated when exposed to the UVA component of sunlight. To achieve this goal, we synthesized a new light-responsive compound by conjugating cholesterol with NBA. Subsequently, this compound, in conjunction with phospholipids, was employed to produce liposomes using the thin-film hydration method. To dual control the drug release pattern and improve the bioavailability of herbal drugs, we encapsulated it inside the cavity of cyclodextrin compounds and then used these drug-loaded cyclodextrin to fabricate liposomes with the drug. The fabricated liposomes had a spherical shape with a size of about 140 nm and a highly negative charge that helped their stability during the storage time. Moreover, they showed a light-responsive drug release pattern after irradiation with 365 nm UV radiation. The results of the cell viability test confirmed their effectiveness against melanoma cancer cells and compatibility with normal cells. These findings underscore the potential of the fabricated liposomes as supplementary agents in sunscreen creams or anticancer hydrogels for skin cancer therapy. However, it is imperative to conduct further research to comprehensively assess their effectiveness and refine their properties.

Author contributions All authors contributed to the study conception and design. Material preparation, data collection and analysis were performed by Ali Zarrabi (A. Z.), Mehmet Yildiz (M. Y.), Arezoo Khosravi (A. Kh.), Yavuz Nuri Ertas (Y. N. E), Atefeh Zarepour (At. Z.), and Zeynep Ülker (Z. U.). The first draft of the manuscript was written by Arezoo Khosravi (A. Kh.), Atefeh Zarepour (At. Z.), and Zeynep Ülker (Z. U.). Scientific revision and grammatical correction were done by Ali Zarrabi (A. Z.), Mehmet Yildiz (M. Y.), Arezoo Khosravi (A. Kh.), and Abdurrahman Coskun (A. C.). All authors read and approved the final manuscript.

Funding Ali Zarrabi acknowledges funding support from the 2535–International Bilateral Cooperation Funding Program of The Scientific and Technological Research Council of Türkiye (TÜBİTAK, Project No: 121N152).

Declarations

Competing interests The authors have no relevant financial or non-financial interests to disclose.

References

1. G. Sanclemente et al., The impact of skin diseases on quality of life: a multicenter study.Actas Dermo-Sifiliográficas (English Edition)**108**(3), 244–252 (2017)
2. E.S. Chambers, M.J.I. Vukmanovic-Stejic, Skin barrier immunity and ageing. Immunology. **160**(2), 116–125 (2020)
3. P.M. Tricarico et al., Aquaporins are one of the critical factors in the disruption of the skin barrier in inflammatory skin diseases. Int. J. Mol. Sci. **23**(7), 4020 (2022)
4. J. Chen et al., Oxidative stress in the skin: Impact and related protection. Int. J. Cosmet. Sci. **43**(5), 495–509 (2021)
5. S.-G. Jin, F. Padron, G.P.J.A. Pfeifer, UVA Radiation DNA Damage Melanoma. ACS omega. **7**(37), 32936–32948 (2022)
6. M. Dildar et al., Skin cancer detection: a review using deep learning techniques. Int. J. Environ. Res. Public Health. **18**(10), 5479 (2021)
7. S. Parham et al., Antioxidant, antimicrobial and antiviral properties of herbal materials. Antioxidants. **9**(12), 1309 (2020)
8. Z. Xu et al., Why traditional herbal medicine promotes wound healing: Research from immune response, wound microbiome to controlled delivery. Adv. Drug Deliv. Rev. **195**, 114764 (2023)
9. Y. Panahi et al., Evidence of curcumin and curcumin analogue effects in skin diseases: a narrative review. J. Cell. Physiol. **234**(2), 1165–1178 (2019)
10. M.C. Fadus et al., Curcumin: an age-old anti-inflammatory and anti-neoplastic agent. J. Traditional Complement. Med. **7**(3), 339–346 (2017)
11. A. Allegra et al., Anticancer activity of curcumin and its analogues: preclinical and clinical studies. Cancer Invest. **35**(1), 1–22 (2017)
12. T. Waghule et al., Emerging trends in topical delivery of curcumin through lipid nanocarriers: effectiveness in skin disorders. Aaps Pharmscitech. **21**, 1–12 (2020)
13. V. Laura et al., Potential. Campione E. Potential of curcumin in skin disorders. Nutrients. **11**(9), 2169 (2019)
14. G. Bozzuto, and A. Molinari, Liposomes as nanomedical devices. Int J Nanomedicine. 975–999 (2015)
15. W. Liu et al., Research progress on liposomes: Application in food, digestion behavior and absorption mechanism.Trends Food Sci. Technol. **104**, 177–189 (2020)
16. M. Dymek, E. Sikora, I., Liposomes as biocompatible and smart delivery systems–the current state. Adv. Colloid Interface Sci. **309**, 102757 (2022)
17. H. Nsairat et al., Liposomes: Structure, composition, types, and clinical applications. Heliyon. **8**(5), e09394 (2022)
18. D.E. Large et al., Liposome composition in drug delivery design, synthesis, characterization, and clinical application. Adv. Drug Deliv. Rev. **176**, 113851 (2021)
19. De V. Leo et al., Liposomes containing nanoparticles: preparation and applications. Colloids Surf B Biointerfaces. **218**, 112737 (2022)
20. D. Guimarães, A. Cavaco-Paulo, E.Nogueira. Design of liposomes as drug delivery system for therapeutic applications. Int. J. Pharm. **601**, 120571 (2021)
21. M. Ashrafizadeh et al., Stimuli-responsive liposomal nanoformulations in cancer therapy: Pre-clinical & clinical approaches. J Control Releas **351**, 50–80 (2022)
22. V.W. Karisma et al., UVA-Triggered drug release and photo-protection of skin. Front. Cell Dev. Biol. **9**, 598717 (2021)
23. G. Hazell et al., Post-exposure persistence of nitric oxide upregulation in skin cells irradiated by UV-A. Sci. Rep. **12**(1), 9465 (2022)
24. M.A. Chaves, S.C. Pinho, Unpurified soybean lecithins impact on the chemistry of proliposomes and liposome dispersions encapsulating vitamin D3. Food Bioscience. **37**, 100700 (2020)
25. Z. Ye et al., Photo-responsive shell cross-linked micelles based on carboxymethyl chitosan and their application in controlled release of pesticide. Carbohydr. Polym.**132**, 520–528 (2015)
26. L. Meng et al., Chitosan-based nanocarriers with pH and light dual response for anticancer drug delivery. Biomacromolecules **14**(8), 2601–2610 (2013)

27. S. Zhou et al., Targeted delivery of epirubicin to tumor-associated macrophages by sialic acid-cholesterol conjugate modified liposomes with improved antitumor activity. Int. J. Pharm. **523**(1), 203–216 (2017)
28. M.H. Ja'far et al., Inclusion of curcumin in β-cyclodextrins as potential drug delivery system: Preparation, characterization and its preliminary cytotoxicity approaches. Sains Malays **47**, 977–989 (2018)
29. J. Chen et al., Characterization of curcumin/cyclodextrin polymer inclusion complex and investigation on its antioxidant and antiproliferative activities. Molecules **23**(5), 1179 (2018)
30. H.K. Syed, K.K. Peh, Comparative curcumin solubility enhancement study of beta-cyclodextrin (beta CD) and its derivative hydroxypropyl-beta-cyclodextrin (HP beta CD). Lat. Am. J. Pharm. **32**(1), 52–59 (2013)
31. C.S. Mangolim et al., Curcumin–β-cyclodextrin inclusion complex: Stability, solubility, characterisation by FT-IR, FT-Raman, X-ray diffraction and photoacoustic spectroscopy, and food application. Food Chem. **153**, 361–370 (2014)
32. P.M. Vyas et al., Synthesis and Characterization of cholesterol nano particles by Using w/o Microemulsion Technique. in AIP Conference Proceedings. 1276, 198-209 (2010)
33. R.M. Silva et al., Preparation of magnetoliposomes with a green, low-cost, fast and scalable methodology and activity study against *S. aureus and C. freundii* bacterial strains. J. Braz. Chem. Soc. **29**, 2636–2645 (2018)
34. F.J. Siyal et al., Eugenol and liposome-based nanocarriers loaded with eugenol protect against anxiolytic disorder via down regulation of neurokinin-1 receptors in mice. Pak. J. Pharm. Sci. **33**, 2275-2284 (2020)
35. S.P. Damari et al., Practical aspects in size and morphology characterization of drug-loaded nano-liposomes. Int. J. Pharm. **547**(1–2), 648–655 (2018)
36. T. Wang et al., Redox-sensitive irinotecan liposomes with active ultra-high loading and enhanced intracellular drug release. Colloids Surf., B **206**, 111967 (2021)
37. E. Tobar-Delgado et al., Enhancing the physicochemical stability and antioxidant activity of cape gooseberry calyx extract through nanoencapsulation in soy lecithin liposomes. Colloids Surf. B: Biointerfaces. **234**, 113662 (2023)
38. T. Naseriyeh et al., Enhanced *in vitro* cytotoxicity and intracellular uptake of Genipin via loaded on Nano-Liposomes made from soybean lecithin in MCF-7 cells. Nanomed. J. **9**(1), 1-10 (2022)
39. R. Gharib et al., Liposomes incorporating cyclodextrin–drug inclusion complexes: current state of knowledge. Carbohydr. Polym. **129**, 175–186 (2015)
40. V.K. Rapalli et al., Curcumin loaded nanostructured lipid carriers for enhanced skin retained topical delivery: optimization, scale-up, in-vitro characterization and assessment of ex-vivo skin deposition. Eur. J. Pharm. Sci. **152**, 105438 (2020)
41. M.-L. Laracuente, M.H. Yu, K.J. McHugh, Zero-order drug delivery: state of the art and future prospects. J. Controlled Release. **327**, 834–856 (2020)
42. N. Saengkrit et al., Influence of curcumin-loaded cationic liposome on anticancer activity for cervical cancer therapy. Colloids Surf., B **114**, 349–356 (2014)
43. M.T. Luiz et al., Folic acid-modified curcumin-loaded liposomes for breast cancer therapy. Colloids Surf. A: Physicochem. Eng. Asp. **645**, 128935 (2022)
44. V. Ravichandiran et al., Quercetin-decorated curcumin liposome design for cancer therapy: in-vitro and in-vivo studies. Curr. Drug Deliv. **14**(8), 1053–1059 (2017)
45. M. Woźniak et al., The comparison of in vitro photosensitizing efficacy of curcumin-loaded liposomes following photodynamic therapy on melanoma MUG-Mel2, squamous cell carcinoma SCC-25, and normal keratinocyte HaCaT cells. Pharmaceuticals. **14**(4), 374 (2021)
46. S.P. Singh et al., NIR triggered liposome gold nanoparticles entrapping curcumin as in situ adjuvant for photothermal treatment of skin cancer. Int. J. Biol. Macromol. **110**, 375–382 (2018)
47. M. Chang, M. Wu, H. Li, Antitumor Effects of Curcumin and Glycyrrhetinic Acid-Modified Curcumin-Loaded Cationic Liposome by Intratumoral Administration, Evidence-Based Complementary and Alternative Medicine. **2020(1)**, 4504936. (2020)
48. Y. Wang et al., Curcumin-loaded liposomes with the hepatic and lysosomal dual-targeted effects for therapy of hepatocellular carcinoma. Int. J. Pharm. **602**, 120628 (2021)
49. A. Zarrabi et al., Synthesis of curcumin loaded smart pH-responsive stealth liposome as a novel nanocarrier for cancer treatment. Fibers. **9**(3), 19 (2021)